Flowfield Measurements for Film-Cooling Holes With Expanded Exits

K. Thole[1]

M. Gritsch

A. Schulz

S. Wittig

Institut für Thermische Strömungsmaschinen, Universität Karlsruhe, Karlsruhe, Federal Republic of Germany

One viable option to improve cooling methods used for gas turbine blades is to optimize the geometry of the film-cooling hole. To optimize that geometry, effects of the hole geometry on the complex jet-in-crossflow interaction need to be understood. This paper presents a comparison of detailed flowfield measurements for three different single, scaled-up hole geometries, all at a blowing ratio and density ratio of unity. The hole geometries include a round hole, a hole with a laterally expanded exit, and a hole with a forward-laterally expanded exit. In addition to the flowfield measurements for expanded cooling hole geometries being unique to the literature, the testing facility used for these measurements was also unique in that both the external mainstream Mach number ($Ma_\infty = 0.25$) and internal coolant supply Mach number ($Ma_c = 0.3$) were nearly matched. Results show that by expanding the exit of the cooling holes, both the penetration of the cooling jet and the intense shear regions are significantly reduced relative to a round hole. Although the peak turbulence level for all three hole geometries was nominally the same, the source of that turbulence was different. The peak turbulence level for both expanded holes was located at the exit of the cooling hole resulting from the expansion angle being too large. The peak turbulence level for the round hole was located downstream of the hole exit where the velocity gradients were very large.

Introduction

New challenges in better turbine blade cooling are ever present with the aim of increasing turbine inlet temperatures to improve gas turbine efficiencies. The attempts in meeting those challenges have focused on improving inner blade convective heat transfer and improving external blade film-cooling. Blade film-cooling is attained by injecting the inner blade convective coolant fluid through the blade surface into the external blade boundary layer.

From a flowfield perspective, ideal film-cooling would occur when a film-cooling jet has minimal penetration into the mainstream such that the jet remains attached to the cooling surface, yet the jet should have a high enough mass flow rate to cover a large area of the blade. Also, the cooling jet should have relatively low turbulent mixing to avoid dilution of the jet by the hot mainstream fluid. In many past studies the focus has been to optimize film-cooling fluid mechanical parameters, such as jet-to-mainstream blowing ratio and momentum flux ratio, for round film-cooling holes that are inclined at nominally 30 deg. Further optimization is still needed. In particular, one viable alternative is to optimize the cooling hole geometry. By gaining a better understanding of the complex flowfield that results from cooling holes that have been laterally and forward-laterally expanded, improvements can be made to the hole geometry to ultimately provide better cooling characteristics of the film.

This paper presents detailed flowfield measurements for three different single, scaled-up, cooling hole geometries for a blowing ratio (M), momentum flux ratio (I), and density ratio (DR) of unity. The three hole shapes include a baseline round hole, a hole with a laterally expanded exit, and a hole with a forward-laterally expanded exit. Thus far, there are no reported detailed flowfield measurements for these hole geometries. This study is also unique because in addition to the mainstream flow, representing the external blade flowfield, there is a parallel flowing coolant supply channel, representing the inner blade convective passage between the midspan and trailing edge of a nozzle guide vane. Thus far, there are no reported detailed flowfield measurements for holes that have both primary and coolant flow passages.

Expanded Cooling Hole Studies

Although it has been over 20 years since Goldstein et al. (1974) first reported their adiabatic effectiveness measurements for laterally expanded cooling holes, there have been relatively few studies reported in the open literature since that time discussing contoured film-cooling holes. Goldstein et al. (1974) showed that by laterally expanding the hole 10 deg, improved adiabatic effectiveness values were measured for a large range of blowing ratios. Specifically, Goldstein et al. showed that for a blowing ratio range between $0.8 < M < 2.2$, the centerline adiabatic effectiveness remained constant at seven hole diameters downstream for the laterally expanded hole. In contrast, they showed for a blowing ratio above $M > 0.3$, the effectiveness dropped significantly for a round hole because of jet detachment. They attributed the improved performance for the laterally expanded hole to the reduced momentum of the exiting jet. A reduction in the exiting jet momentum can be achieved for the same jet mass flow rate by expanding the cooling hole exit area.

In a later study, Makki and Jakubowski (1986) measured higher adiabatic effectiveness values for a forward-laterally expanded hole in comparison to a round hole. Sen et al. (1996) showed that improved cooling performance at a high momentum flux ratio ($I = 3.9$) could also be obtained for a 60 deg compound angle hole when the hole had a forward expansion. Compound angle holes refer to holes that inject the coolant laterally with respect to the mainstream. Without the forward

[1] Present address: Department of Mechanical Engineering, University of Wisconsin, Madison, WI 53706-1572.

Contributed by the International Gas Turbine Institute and presented at the 41st International Gas Turbine and Aeroengine Congress and Exhibition, Birmingham, United Kingdom, June 10–13, 1996. Manuscript received at ASME Headquarters February 1996. Paper No. 96-GT-174. Associate Technical Editor: J. N. Shinn.

expansion, Sen et al. (1996) showed that the film-cooling was completely ineffective.

Flowfield Structures of Film-Cooling Jets

Past flowfield investigations have given some physical insight as to the primary flow structures dictating the interaction between the cooling jet and the mainstream crossflow for a round hole geometry. These flowfield investigations include those of Yoshida and Goldstein (1984), Jubran and Brown (1985), Pietrzyk et al. (1989), Subramanian et al. (1992), Benz et al. (1993), Leylek and Zerkle (1993), Lee et al. (1994) and Garg and Gaugler (1995). At high blowing ratios, $M \geq 1$, the dominating flow structures for a round hole film-cooling jet include a separation region which forms at the inlet of the cooling hole, intense shear regions as the mainstream interacts with the jet, and longitudinal vortices that form at the lateral edges of the jet.

The formation of a separation region was first identified by Pietrzyk et al. (1989) to occur at the hole entrance on the leeward side of the hole. In the Pietrzyk et al. (1989) study, the coolant was supplied by a plenum and as a result the flow encountered a large turning angle on the leeward side of the hole, which caused a separation region. This separation region skewed the exiting jet toward the windward side of the hole. Benz et al. (1993), Leylek and Zerkle (1993), and Garg and Gaugler (1995) also discuss the importance of numerically simulating the jet flow inside the cooling hole to achieve realistic exiting conditions. In addition to skewing the jet, the separation region causes high turbulence levels in the exiting jet, which promotes turbulent mixing and jet dilution.

Upstream of the obstructing jet, the external boundary layer encounters a large blockage effect decelerating the boundary layer. At the upstream hole edge, the jet velocity is faster relative to the mainstream boundary layer, which then produces an intense shear region.

Based on detailed flowfield measurements, Andreopoulos and Rodi (1984) first identified counterrotating vortices in their study of a normal jet issuing into a mainstream. Similarly for an inclined film-cooling jet, measurements presented by Pietrzyk (1989) and Subramanian et al. (1992) showed a pair of counterrotating vortices that entrain "hot" mainstream fluid and transport that fluid toward the blade surface.

Based on these flowfield characteristics, it was the intent of this investigation to determine the effect of the hole geometry on this complex flowfield in order to improve upon the overall heat transfer characteristics of a film-cooling jet. In particular, the primary improvements to the film cooling process can be made by insuring the jet remains attached to the surface, by eliminating the counterrotating vortices, and by minimizing the velocity gradients. The remainder of this paper discusses the experimental facility and instrumentation used for this investigation and the flowfield mappings for three different geometric cooling holes.

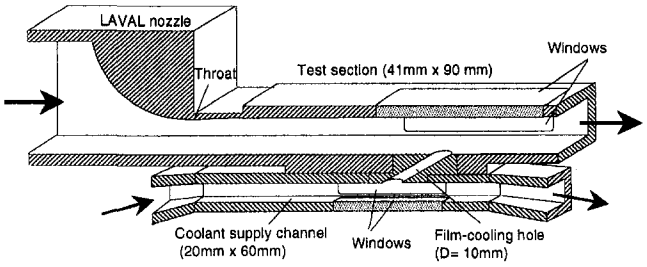

Fig. 1 Schematic of the film-cooling test section

Experimental Facility and Instrumentation

The experiments discussed in this paper were conducted in a new test facility at the Institut für Thermische Strömungsmaschinen, Universität Karlsruhe, which is described in detail by Wittig et al. (1996). A sketch of the test section is shown in Fig. 1. Mainstream and coolant flow channels, which can be independently controlled, were included in the test facility to simulate the flowfields associated with external and internal blade cooling. The flow conditions in the primary and coolant channels are given in Table 1. The blowing ratio for each of the three holes tested was $M = 1$ at a density ratio of $DR = 1$.

The air for both flow channels was supplied by a large compressor that has a capacity of producing 1 kg/s at a pressure of 11 bar. Flow for the coolant channel was also provided by the compressor, but driven through the secondary flow loop by a sealed external blower.

Table 1 Flow conditions for primary and coolant channels

	Primary Channel	Coolant Channel
Mach Number	0.25	0.30
Mean Freestream Velocity (m/s)	85.0	102.7
Freestream Turbulence Intensity(%)	1.5	1.0
Stagnation Pressure (Bars)	1.05	1.05-1.09
Total Temperature at Injection (K)	300	300
Re_D	5.2×10^4	6.6×10^4
δ_{99}/D at x/D = -2	0.8	
δ_{99}/D at x/D = -7		0.2
Re_θ at x/D = -2	3800	

Nomenclature

D = cooling hole diameter at hole inlet
DR = jet-to-mainstream density ratio
I = jet-to-mainstream momentum flux ratio = $\rho_j V_j^2 / \rho_\infty V_\infty^2$
L = cooling hole length along centerline axis
M = jet-to-mainstream blowing or mass flux ratio = $\rho_j V_j / \rho_\infty V_\infty$
Ma = Mach number
Re_D = hole diameter Reynolds number
Re_θ = momentum thickness Reynolds number
Tu = turbulence intensity = $100 \cdot \sqrt{0.5(u'^2 + v'^2)}/U_\infty$
Tu_j = turbulence intensity inside hole = $100 \cdot \sqrt{u'^2}/V_j$
u', v', w' = streamwise, vertical, and lateral rms velocities
U, V, W = streamwise, vertical, and lateral mean velocities
$\rho\overline{u'v'}$ = turbulent shear stress components
$\rho\overline{u'^2}$, $\rho\overline{v'^2}$ = turbulent normal stress components
V_j = total jet velocity using hole inlet and mass flux
x = streamwise distance based on hole centerline
y = vertical distance based on exit of hole
z = spanwise distance based on hole centerline
δ_{99} = boundary layer thickness, 99 percent point
θ = momentum thickness
ρ = density

Subscripts and Superscripts

ex = exit conditions
j = jet conditions
∞ = mainstream conditions

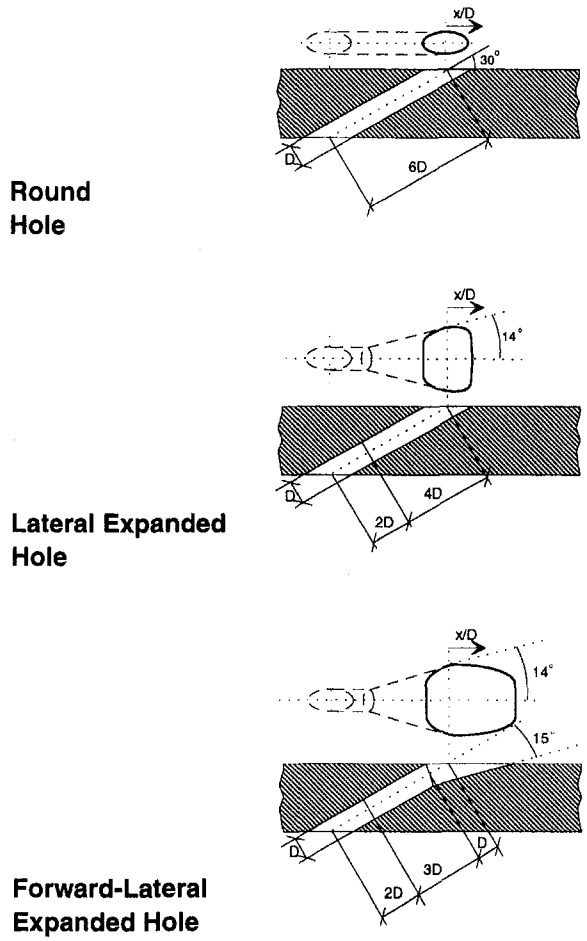

Fig. 2 Film-cooling hole geometries

The flow rate in the coolant channel was 0.12 kg/s and, at a blowing ratio of unity, the flow rate through the cooling hole was 7.5e-03 kg/s. As a result of the large disparity between the two flow rates, high uncertainties would occur if the flow rates upstream and downstream of the cooling hole were measured using the continuity equation to determine the blowing ratio. To reduce the uncertainty, the blowing ratio of the cooling hole was set by measuring the coolant mass flow entering the coolant channel. Leak tests were conducted on the coolant supply channel to insure that all of the mass flow rate entering the coolant channel was exhausted only through the cooling hole. The coolant channel flow was considered to be a boundary layer flow with a thickness of $\delta_{99} = 2$ mm as compared to a channel half-height of 10 mm at a location of seven hole diameters upstream of the hole inlet.

The three single, scaled-up hole shapes that were investigated are shown in Fig. 2. These hole geometries were obtained in cooperation with several European gas turbine companies. The diameter of all three holes at the inlet was 10 mm. These holes were machined into flat aluminum test plates 30 mm thick. All three holes were inclined at 30 deg, giving a length-to-hole diameter ratio of $L/D = 6$, where L is measured along the hole centerline axis at the hole inlet. The lateral expansion angle, which started two hole diameters after the hole inlet for the two contoured holes, was 14 deg. The forward expansion angle for the forward-laterally expanded hole was 15 deg relative to the hole centerline axis and started five hole diameters after the hole inlet. The streamwise distance, x, also shown in Fig. 2, had the origin at the hole centerline axis just at the exit of the hole. The length of the round and lateral expanded holes, as viewed from above the hole exit, extended two hole diameters in the streamwise direction. The length of the forward-lateral expanded hole extended four hole diameters.

A two-component, coincident, fiber optic laser-Doppler velocimeter (LDV) was used to measure velocity fields for the three shaped holes. The commercial LDV system was an 85 mm fiber optic probe from Dantec. The processors used were Dantec's Enhanced Burst Spectrum Analyzers. The probe volume size was reduced, using a beam expander, to a diameter of 74 μm and a length of 0.6 mm. The LDV was rotated at 45 deg and tilted at nominally 4.5 deg to allow near-wall measurements. As a result of the tilt, the vertical velocity, v, reported in this paper contains a small lateral velocity component. The tilt does not affect the streamwise velocity component. The data were post-processed using a 2 μs coincident window and bias corrected using residence time weighting. Both the primary and coolant channel flows were seeded with oil (DES) particles having a mean diameter of 0.5 μm. Because the coolant channel and primary flow were at different pressures, valves were used downstream of the seeder such that the seeding injection was independently controlled to avoid velocity biases.

Vertical velocity profiles were taken at 14 streamwise locations at the streamwise centerline of the cooling holes. Vertical velocity profiles were taken at seven spanwise positions on one side of the cooling hole at $x/D = 4$ to compare the lateral spreading of the jet.

Uncertainty Estimates

Based on a 95 percent confidence interval, both bias and precision uncertainties were quantified. The data presented in this paper were typically averaged over 10,000 points or more depending on the data rate. The bias uncertainty for the mean velocities was 0.4 percent, whereas the precision uncertainties were 1 percent in the free stream and 3.4 percent near the wall. The precision uncertainty for the rms velocity measurements was 1.4 percent in the free stream and 5.8 percent near the wall. The precision uncertainty in the turbulent shear stress was 5.6 percent. Positioning uncertainty of the LDV probe volume with respect to the hole was $\Delta x = \pm 0.05$ mm, $\Delta y = \pm 0.05$ mm, and $\Delta z = \pm 0.05$ mm. The uncertainty in setting the coolant mass flow rate was 2 percent.

Results

Although flowfield measurements have previously been reported for round holes, as mentioned in the introduction, there have not been any reported flowfield studies in the open literature that have used a round hole geometry with a flowing coolant supply channel at the hole inlet. Prior to presenting the results with a flowing coolant supply, a benchmark comparison was made by turning off the blower that drives the coolant supply channel. By turning off the blower, the coolant channel was operated as a plenum supplying the cooling hole. Comparisons could then be made to data presented by Pietrzyk et al. (1989), who used a plenum. As can be seen in Fig. 3, the centerline velocity profiles at $x/D = 3$ agree fairly well. The differences between the data can be attributed to the present study having a larger hole length-to-diameter ratio of $L/D = 6$ relative to that of Pietrzyk et al. (1989) who used an $L/D = 3.5$, and the angle for the Pietrzyk et al. data was slightly steeper at 35 deg.

The following sections present the mean flowfield results and turbulent flowfield results for all three hole geometries at a blowing ratio of $M = 1$. Velocity contours inside the cooling hole plane will be presented. This discussion will be followed by a discussion on the flowfield between $-2 < x/D < 10$ in a vertical streamwise plane at the hole centerline and in a vertical-lateral plane at a streamwise location of $x/D = 4$.

Film-Cooling Hole Flowfield

By mounting the LDV fiber optic probe above the test section, it was possible to measure the streamwise velocity components

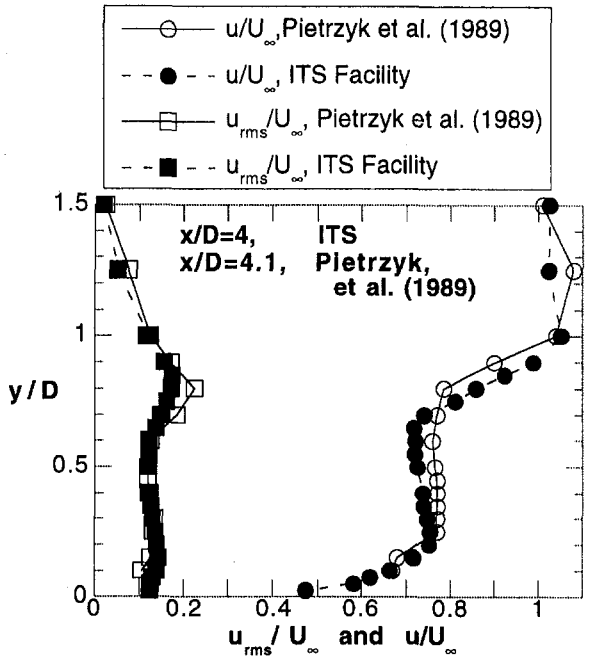

Fig. 3 Comparison of mean and rms velocity data with those presented in the literature at $M = 1$ and $DR = 1$

inside the film-cooling hole. These measurements were made in a vertical spanwise plane at $x/D = -0.75$, which corresponds to just 0.25D downstream of the windward start of the cooling hole. Note that this location is much downstream of the start of the lateral expansion in both of the expanded holes, but is still upstream of the start of the forward expansion for the forward-lateral expanded hole.

Figure 4 compares streamwise velocity contours inside the cooling hole for the three different hole geometries. For the round hole, the highest velocities are found in the center of the cooling hole. The differences between these measurements and those numerical predictions presented by Leylek and Zerkle (1993), in which the highest speed fluid was predicted to occur on the top of cooling hole (windward side of the cooling hole), can be attributed to the differences between the jet coolant supply. In the study of Leylek et al., the coolant was supplied by a stagnant plenum, whereas in the present configuration, the jet fluid was supplied by a crossflow at the entrance. As described by Thole et al. (1997), the presence of the crossflow at a round hole entrance can have a major influence on the coolant jet.

The streamwise velocity contours for the cooling holes with the expanded exits, also shown in Fig. 4, indicate the highest velocities occurring near the bottom and in the spanwise center of the cooling holes. There is little or no jet fluid occurring at the top of both the holes. The laterally-expanded hole does show slightly less variation in the spanwise direction, or rather the coolant does expand to fill the hole slightly better than the forward-lateral hole.

Figure 5 shows the turbulence level contours for the three hole geometries at $x/D = -0.75$ inside the coolant hole. The turbulence levels are based on the rms of the streamwise velocity fluctuations and the total jet velocity as calculated from the blowing ratio ($Tu_j = u'/V_j$). These results indicate much higher turbulence levels occuring inside the coolant hole for the two expanded cooling holes, 12 percent $< Tu_j <$ 20 percent, than for the round hole, 6 percent $< Tu_j <$ 12 percent.

Mean Flowfield Results

Normalized mean velocity vectors in the near-hole region for the round, laterally expanded, and forward-laterally expanded hole geometries are shown in Fig. 6. The upstream and downstream edges of the holes are indicated by the lines placed below the x axis.

At the leading edge of the cooling hole ($x/D = -1$), the round hole geometry shows a larger deceleration in the near-wall region as compared to both the expanded holes, indicating a more severe blockage effect. In the case of the round hole, just downstream of the leading edge of the hole at an $x/D = -0.5$, an upward penetration can already be detected. Farther downstream but still over the hole exit, the velocity vectors for the round hole show a stronger penetration relative to either of the expanded holes. In the case of the laterally expanded hole, it is not until the hole centerline ($x/D = 0$) that the streamlines indicate an upward motion. In the case of the forward-lateral expanded hole, the vertical deflection is even less, as indicated by the only slightly positive vertical velocity vectors starting at the hole centerline ($x/D = 0$). Because the jet-to-free stream momentum at the hole exit is the highest for the round hole relative to the expanded holes, there is a stronger penetration of the jet into the boundary layer. The jet-to-mainstream momentum flux ratio at the hole exit is $I_{ex} = 1$ for the round hole, whereas at the exit of the two expanded holes, the momentum flux ratio is $I_{ex} = 0.25$ (based on the area perpendicular to the hole centerline axis measured where the upstream edge of the hole hits the top of the test plate). Although the momentum flux ratio is nominally the same for both the lateral and forward-lateral holes at the hole exits, the forward expansion reduces the jet penetration relative to the laterally expanded hole.

Upstream of the hole centerline between $-1 < x/D < -0.5$ for the forward-laterally expanded hole, the measured vertical

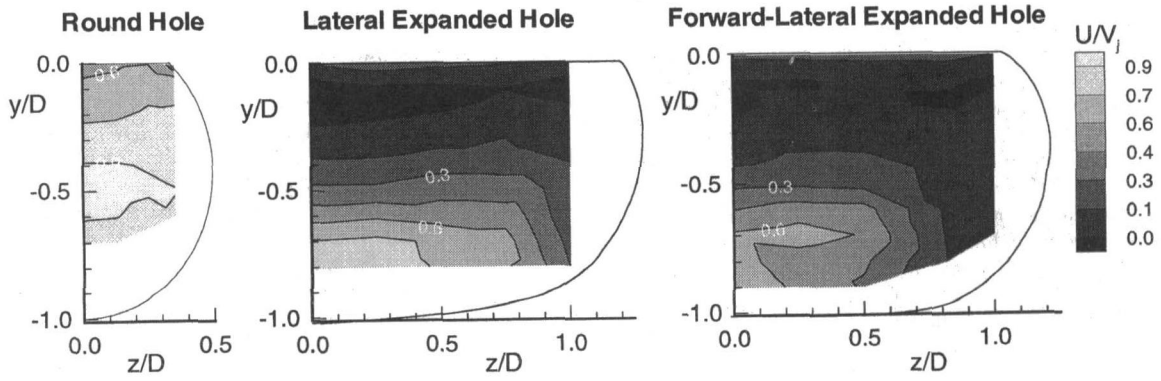

Fig. 4 Streamwise velocity contours inside the coolant hole at $x/D = -0.75$ for the (*a*) round, (*b*) laterally expanded, and (*c*) forward-laterally expanded holes

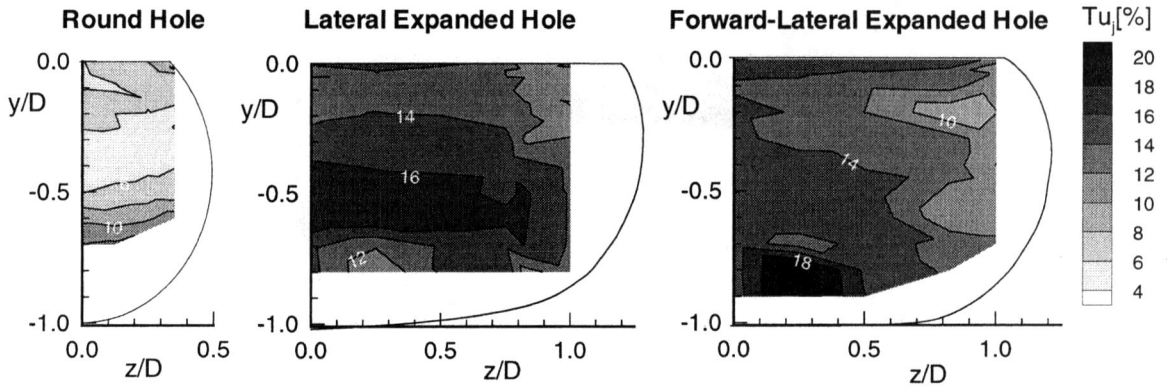

Fig. 5 Jet turbulence level contours inside the coolant hole at $x/D = -0.75$ for the (*a*) round, (*b*) laterally expanded, and (*c*) forward-laterally expanded holes

velocities, although quite low in magnitude, were negative in sign, indicating that some of the mainstream fluid is being ingested into the leading edge of the hole. From the standpoint of cooling, ingestion of the hot mainstream into the coolant hole would produce an overall lower possible cooling effectiveness. Measurements of the vertical velocity component for both the round hole and the laterally expanded hole were positive along the entire jet exit centerline.

Figures 7 and 8 compare the mean streamwise and vertical velocity components for all three holes geometries at three streamwise positions, $x/D = 0$, 2, and 10. As a point of reference, also shown in Fig. 7 is the one-seventh power law for turbulent boundary layer with no injection. At the hole centerline ($x/D = 0$) of the round hole, the formation of a shear layer is indicated by a negative velocity gradient near the hole exit. The negative velocity gradient indicates a jet velocity that is slightly higher than the mainstream at the exit of the cooling hole. The velocity profile for the laterally expanded hole indicates essentially a zero velocity gradient near the hole exit and no formation of a negative velocity gradient shear layer. For the forward-laterally expanded hole, the jet exits primarily from the downstream portion of the hole and, thus, at the hole centerline only a slight deceleration with respect to a turbulent boundary layer is detected. As expected, a higher vertical mean velocity component, shown in Fig. 8, occurs for the round hole relative to the expanded holes at the hole centerline.

The intense shear layers for a round film cooling hole geometry are quite evident at an $x/D = 2$, as shown in Fig. 7(*b*).

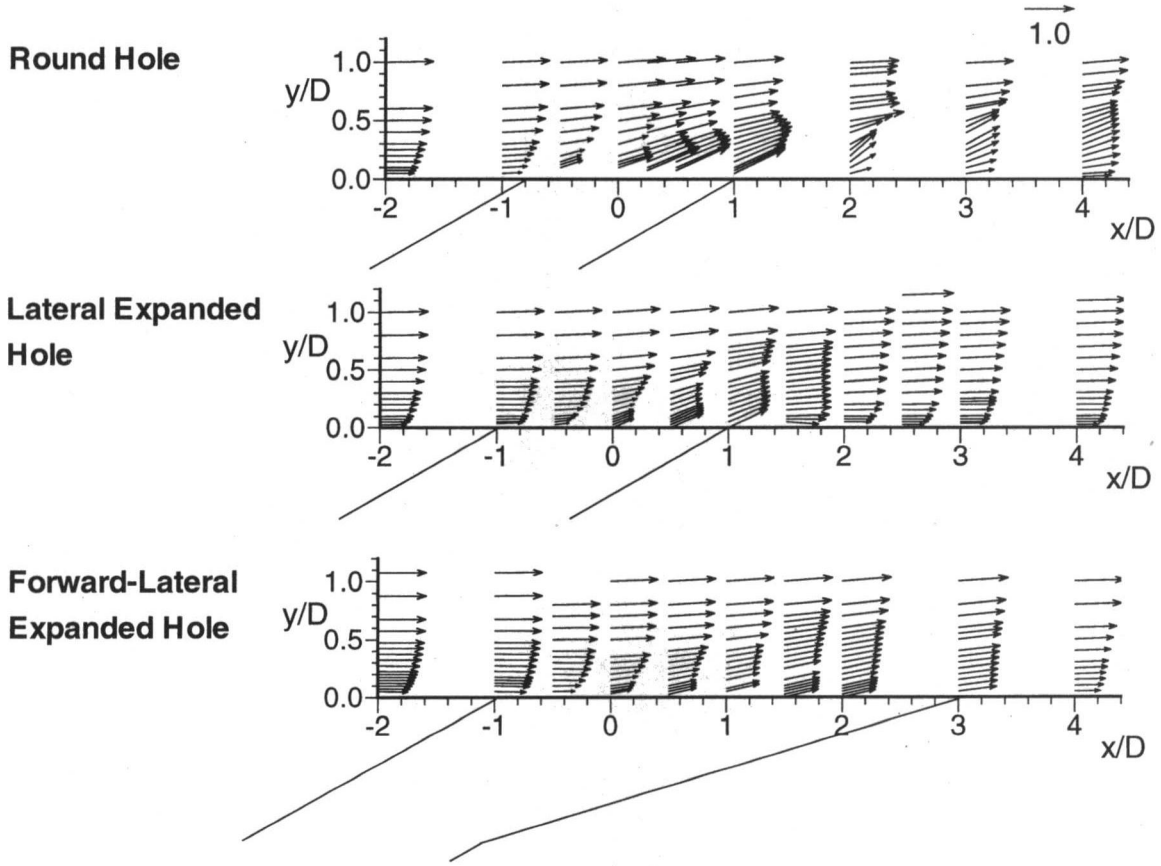

Fig. 6 Mean velocity vectors for the (*a*) round, (*b*) laterally expanded, and (*c*) forward-laterally expanded cooling holes

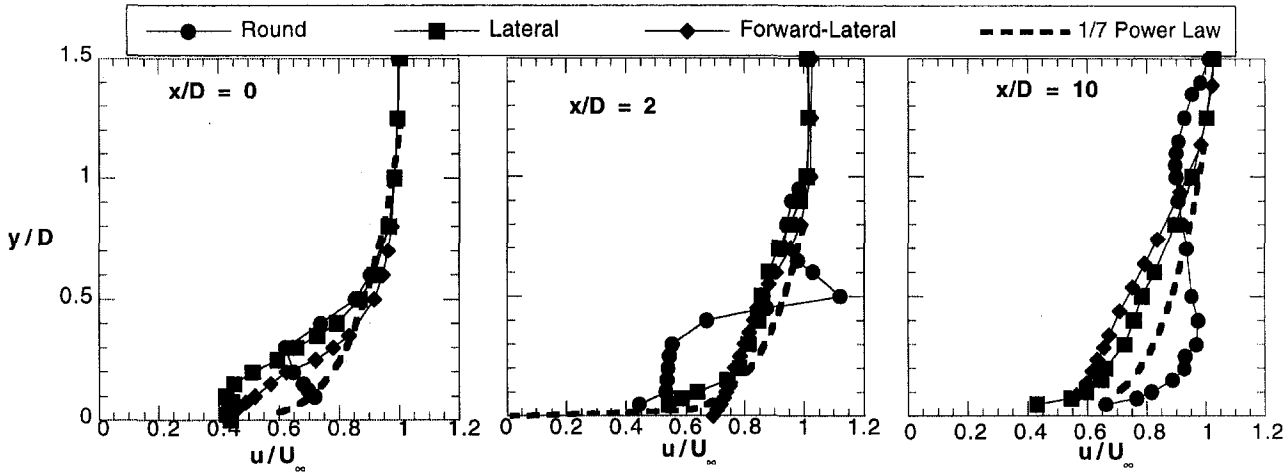

Fig. 7 Mean streamwise velocity profiles for all three hole geometries at (*a*) $x/D = 0$, (*b*) $x/D = 2$, and (*c*) $x/D = 10$

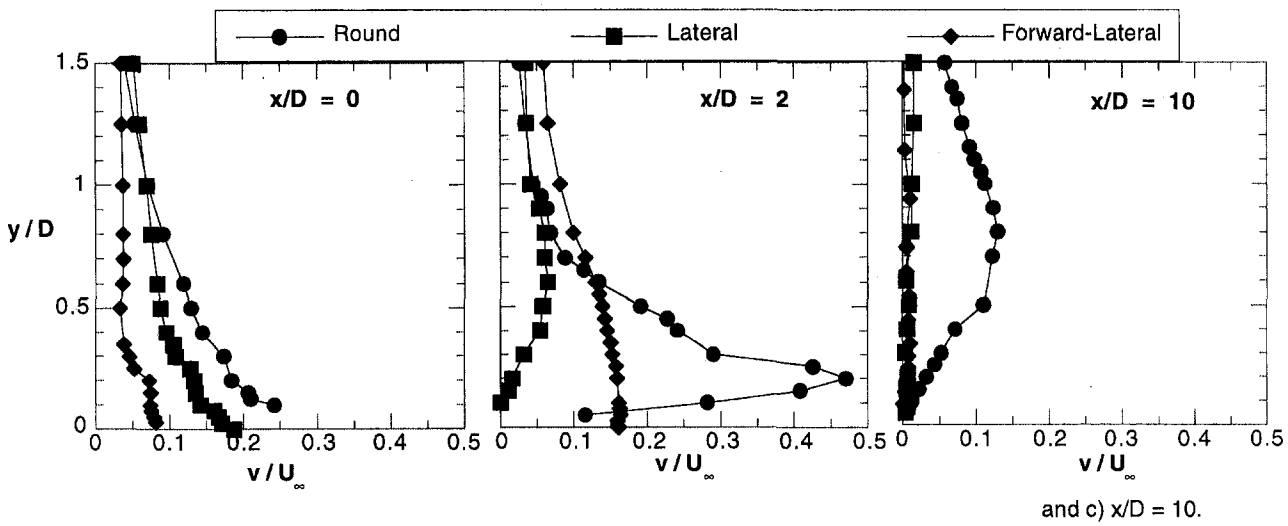

and c) x/D = 10.

Fig. 8 Mean vertical velocity profiles for all three hole geometries at (*a*) $x/D = 0$, (*b*) $x/D = 2$, and (*c*) $x/D = 10$

Note that the peak mean streamwise velocity is $u/U_\infty = 1.2$ and greater than unity as a result of the skewed exiting jet profile. This is similar to those results already presented in the literature in Fig. 3. This streamwise location is one hole diameter beyond the downstream hole edge for both the round and laterally expanded cooling holes and is still over the hole exit for the forward-laterally expanded cooling hole. The shear layer forming at the windward side of the cooling hole, as discussed above, is clearly evident for the round hole at a $y/D = 0.5$. In the case of both expanded holes, there is no indication of the formation of a strong shear layer. In particular, the velocity profile for the forward-laterally expanded hole is relatively flat all the way down to the hole exit. The vertical velocity component of the round jet is much higher than that of the expanded holes as seen in Fig. 8(b). Because the jet primarily exits from the downstream portion of the forward-laterally expanded hole, a larger vertical velocity component was measured relative to the laterally expanded hole at an $x/D = 2$.

Remnants of the upstream shear layer, as indicated in Fig. 7(c), are still evident at an $x/D = 10$ for the round hole. The streamwise velocity profile for the round hole indicates a larger velocity in the near-wall region, between $0 < y/D < 1$, than for the expanded holes. These higher velocities also represent a larger overall massflow in the near-wall region. One plausible explanation for the higher massflow is due to the mainstream entrainment by the longitudinal vortices. Since only two components of velocity were measured, longitudinal vortices could not be quantified in this study. However, comparisons of the vertical velocity components measured in a lateral-vertical plane at $x/D = 4$ are consistent with the presence of longitudinal vortices for the round hole geometry. At an $x/D = 4$ for the round hole geometry, positive vertical velocities were measured at the hole centerline and negative vertical velocities were measured at the outer edges of the jet. In comparison, the vertical velocity component for both the laterally expanded and forward-laterally expanded holes indicated only a slightly positive vertical velocity at the jet centerline and no negative velocities at the jet edges. These results indicate that strong counterrotating vortices do not exist at an $x/D = 4$ for either of the expanded holes. Figure 8(c) shows the continued presence of a higher vertical velocity component for the round hole relative to the expanded holes at an $x/D = 10$.

The spreading of the jet can be seen from the streamwise velocity contours presented in Fig. 9, which were measured in a vertical-lateral plane at an $x/D = 4$. Whereas the laterally and forward-laterally expanded holes show relatively uniform spanwise velocity contours, the round hole still has characteristics of a round jet.

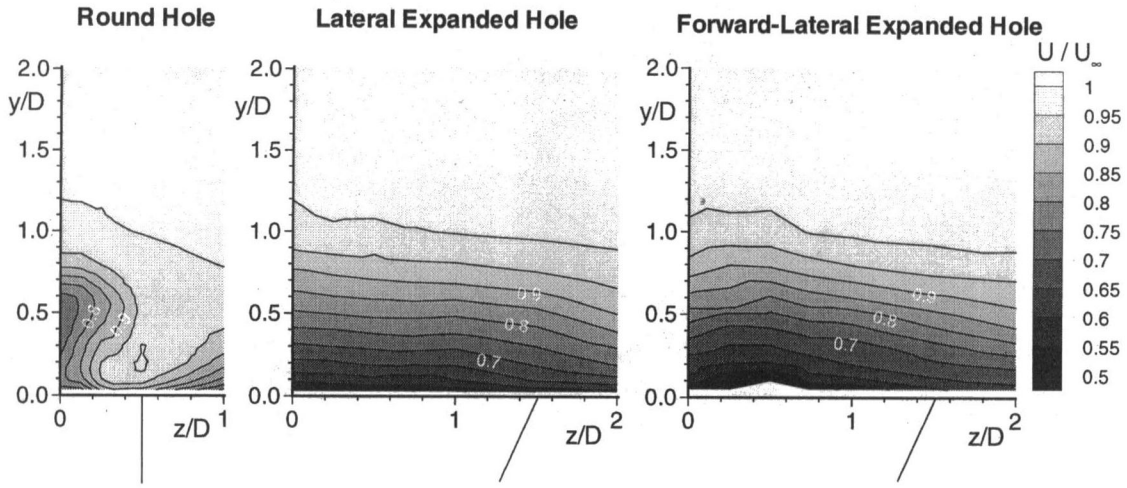

Fig. 9 Comparison of the mean streamwise velocity contours at an $x/D = 4$ for the (*a*) round, (*b*) laterally expanded, and (*c*) forward-laterally expanded holes

Turbulent Flowfield Results

Before comparing the turbulent fields for these three geometries, it is important to recognize differences between a round hole with a flowing supply channel and a round hole with a plenum supply. As indicated in the introduction, past studies have identified the formation of a separation region on the leeward side of the cooling hole inlet, causing the exiting jet to be skewed toward the upstream edge of the hole at high blowing ratios ($M = 1$). The formation of this separation region was consistent with the high turbulence levels exiting the hole. A separation region occurs for a plenum condition because a large turning angle is required on the leeward side of the hole entrance. In the present configuration where the mainstream flow and coolant supply flow are both flowing in the same direction, it is expected that if there is a separation region, it would most likely occur on the upstream edge of the round hole entrance. However, based on the low turbulence intensities measured inside the round hole and at the exit plane of the hole for these flow conditions, a separation region was not apparent.

Previous experiments completed by Pietrzyk et al. (1989) discuss the relationship between mean velocity gradients and both the normal and shear stress production. As already discussed, the streamwise mean velocity gradients for the round hole geometry are much larger than for the expanded cooling holes.

Turbulence level contours in the near-hole region for all three hole geometries are shown in Fig. 10. The peak turbulence levels for the round, laterally expanded, and forward-laterally expanded cooling holes are Tu = 19.5, 18, and 17 percent, respectively. Although the peak turbulence levels for all three holes are comparable, the location of the peak turbulence level is quite different for the round hole as compared to the expanded holes. In the case of the round hole, the peak turbulence level is downstream of the hole exit at $x/D = 2$ as shown in Fig. 10(a). In the case of the expanded holes, the peak turbulence level and turbulent shear stress occurs over the hole exit as shown in Figs. 10(b) and 10(c). Since the inlet geometry and flow conditions for all three holes are the same and since the turbulence levels exiting the round hole are quite low, thereby indicating no separation region inside the round hole, it can be expected that the expanded holes also have no separation region at the hole inlets. However, high turbulence levels do occur at the exits of the expanded holes. These high turbulence levels are a result of having a lateral expansion angle too large thereby allowing the jet to separate from the side walls. Recall, the lateral expansion half angle is 14 deg.

Not only do the high turbulence levels begin at a location farther downstream for the round hole relative to the expanded holes, the extent of the high turbulence region is over a much larger surface area. Turbulence levels as high as 18 percent are shown between $1.5 < x/D < 3.5$ for the round hole, whereas for the laterally expanded hole the high-turbulence regions extend only over half of the hole exit. Because of the absence of strong shear layers for the expanded holes, there is no sustenance for the turbulence production over a region beyond the exit of the hole.

The turbulence level contours in Fig. 11 are for the vertical-lateral plane at an $x/D = 4$. At this location the turbulence levels for both the expanded holes are much less than the round hole and, again, the jet characteristics are still evident for the round hole. The turbulence levels are slightly higher for the forward-laterally expanded jet because this location is only one hole diameter downstream of the hole edge.

Figure 12 shows the turbulent shear stress contours in the near-hole region for the three hole geometries. The peak magnitudes of the turbulent shear stress for the round, lateral expanded, and forward-lateral expanded holes are $\overline{u'v'}/U_\infty^2 = -0.014$, -0.016, and -0.015, respectively. There is a relatively good correspondence between the location of peak turbulence level (normal stress) and peak turbulent shear stress for all three hole geometries. Again, the peak shear stress levels are similar in magnitude and sign for the three holes but the locations are much different.

These measurements indicate a good correspondence between mean gradients and the peak stress locations. In the case of the round hole, the peak location is at $x/D = 2$, as shown in Fig. 12(a), which corresponds to a location of a large positive streamwise velocity gradient ($\partial U/\partial y$) and a large negative vertical velocity gradient ($\partial V/\partial y$) both of which contribute to a negative $\overline{u'v'}$ production. Positive normal stress production ($\overline{u'^2}$) occurs when the streamwise velocity gradient ($\partial U/\partial y$) and turbulent shear stress ($\overline{u'v'}$) are opposite in sign, which coincides with the peak shear stress location. Similarly, in this region the vertical velocity gradient ($\partial V/\partial y$) is negative giving a positive normal stress production of $\overline{v'^2}$.

Results reported by Pietrzyk et al. (1989) showed relatively high positive $\overline{u'v'}$ values exiting the windward side of the round cooling hole similar to those shown in Fig. 12(a). However, unlike Pietrzyk et al., who showed $\overline{u'v'}$ values equal in magnitude but opposite in sign exiting on the downstream portion of the hole, these measurements show relatively low negative $\overline{u'v'}$ values exiting the downstream portion of the hole. This difference can be attributed to the separation region inside the coolant hole.

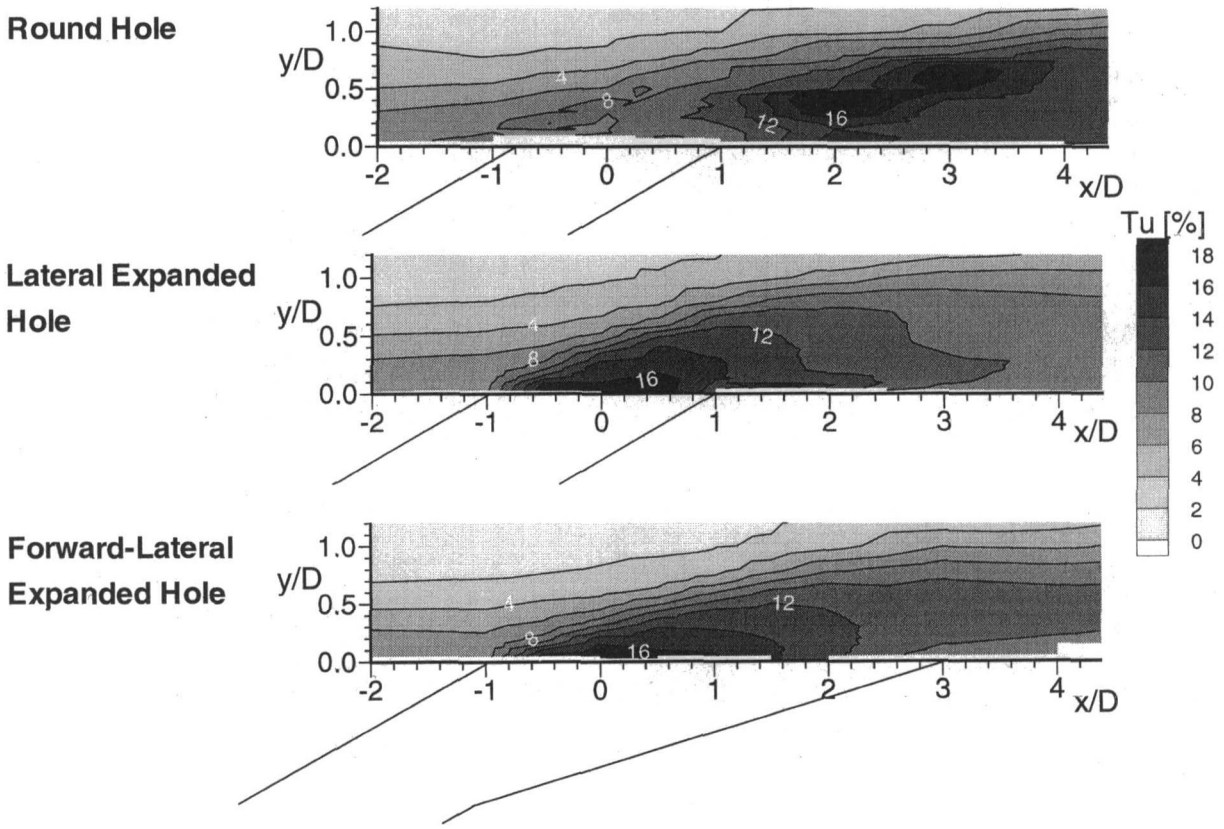

Fig. 10 Turbulence level contours for the (*a*) round, (*b*) laterally expanded, and (*c*) forward-laterally expanded cooling holes

For both expanded holes, high negative $\overline{u'v'}$ values occur at the upstream portion of the cooling hole and relatively high positive $\overline{u'v'}$ values occur in the downstream portion of the cooling hole as shown in Figs. 12(*b*) and 12(*c*). In both the upstream and downstream regions of the expanded cooling holes, there is a relatively small vertical velocity gradient ($\partial V/\partial y$) and large positive streamwise velocity gradients ($\partial U/\partial y$) with the latter dictating the shear stress production. The positive $\overline{u'v'}$ values exiting the lee of the jet are lower in magnitude because of the reduced velocity gradients inside the expanded holes.

Conclusions

Flowfields for three different film-cooling hole geometries have been measured and compared at a blowing ratio of $M = 1$. Past heat transfer studies have indicated that by laterally expanding the exit of the hole, higher effectiveness values could be obtained over a wide range of blowing ratios (Goldstein et al., 1974). From a cooling standpoint, expanding the hole exit as much as possible also allows for greater blade surface coverage.

In comparing both the expanded hole flowfields with the round hole flowfield, the jet penetration as well as the velocity

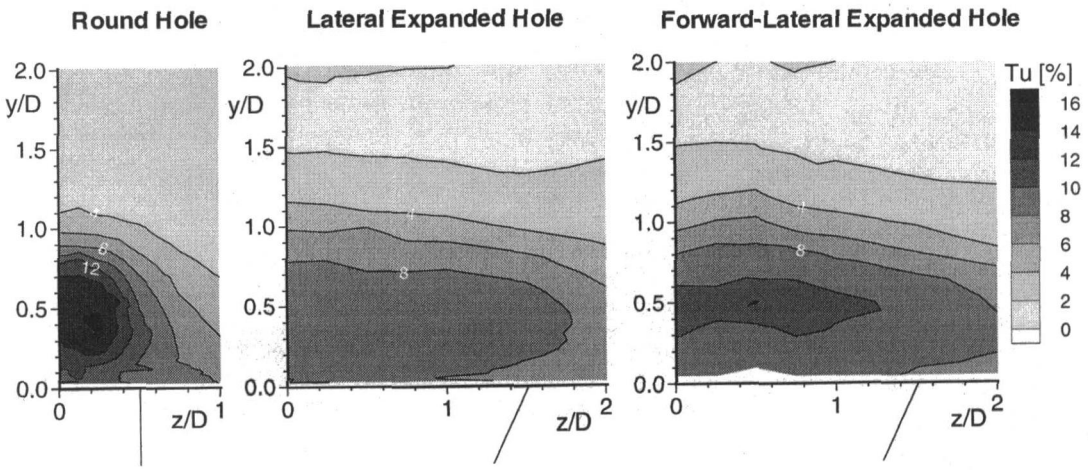

Fig. 11 Turbulence level contours at an $x/D = 4$ for the (*a*) round, (*b*) laterally expanded, and (*c*) forward-laterally expanded cooling holes

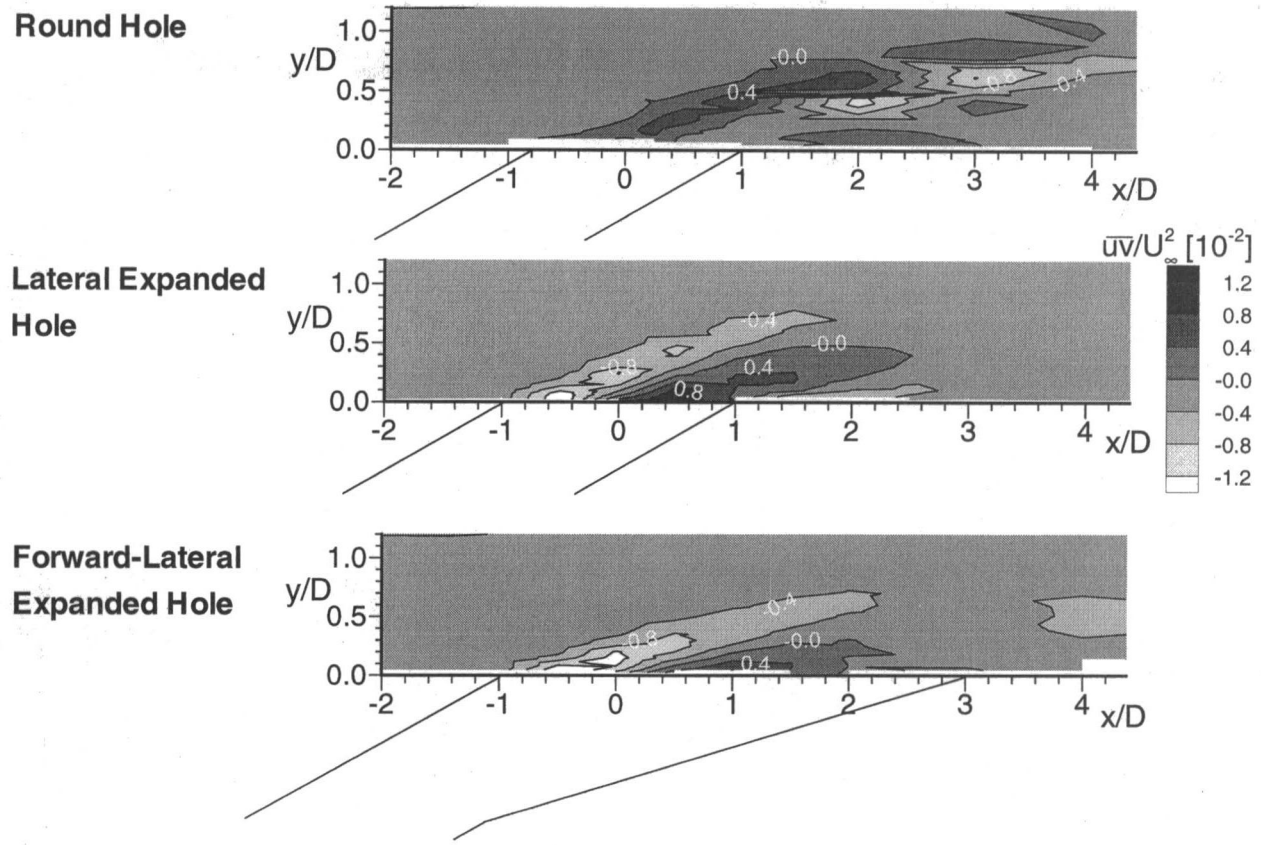

Fig. 12 Turbulent shear stress contours for the (*a*) round, (*b*) laterally expanded, and (*c*) forward-laterally expanded holes

gradients were significantly reduced for the laterally and forward-laterally expanded holes. Because the velocity gradients were reduced by expanding the cooling holes, the turbulence production downstream of the expanded holes was quite low relative to the round hole. The peak turbulence levels for both the expanded holes occurred over the hole exit, whereas the peak level for the round hole occurred downstream of the hole exit where the velocity gradients were very large. The high levels of turbulence exiting the expanded cooling holes resulted from having large expansion angles. Improved cooling performance for the expanded holes can be expected because of reduced jet penetration and because there was no indication of a strong vortical motion occurring at $x/D = 4$. Based on the flowfield measurements, the primary improvement to the expanded holes is to reduce the expansion angle with the tradeoff being a reduced lateral coverage.

Both the laterally expanded and forward-laterally expanded flowfields were quite similar in terms of velocity gradients. The primary disadvantage, however, for the forward-laterally expanded hole is that even though the blowing ratio was quite high, the jet exits primarily from the leeward side of the cooling hole, thereby allowing ingestion of the mainstream fluid into the windward side of the cooling hole. This ingestion would reduce the performance of the film-cooling jet.

In comparing the performance of each of the three hole geometries, this study has reaffirmed the importance of understanding how the jet forms inside the film-cooling hole for all hole geometries. The location and duration of the peak turbulence levels, which dictate the dilution of the cooling jet, depend upon what happens inside the cooling hole. As shown by previous investigators, the peak turbulence level at high blowing ratios for a round hole geometry occurs at the exit of the cooling hole. These turbulence levels result from a large separation region inside the hole that occurs due to the coolant fluid being supplied by a stagnant plenum. Lower turbulence levels over the cooling hole exit (relative to previous studies) were presented in this paper for a round cooling hole that was supplied by a channel flowing parallel to the mainstream. These low turbulence levels indicate the lack of a (or only a small) separation region.

Acknowledgments

This study was partly funded by the European Union through a grant by the Brite Euram program "Investigation of the Aerodynamics and Cooling of Advanced Engine Turbine Components" under Contract No. AER2-CT92-0044. The authors wish to express their gratitude to the partners involved in the program for the permission to publish this paper and to R. Clifford from Rolls-Royce, who coordinated the program.

References

Andreopoulos, J., and Rodi, W., 1984, "Experimental Investigation of Jets in a Crossflow," *Journal of Fluid Mechanics,* Vol. 138, pp. 93–127.

Benz, E., Wittig, S., Beeck, A., and Fottner, L., 1993, "Analysis of Cooling Jets Near the Leading Edge of Turbine Blades," 72nd Fluid Dynamics Panel Meeting and Symposium on "Computational and Experimental Assessment of Jets in Cross Flow," Winchester, UK, Paper No. 37.

Garg, V., and Gaugler, R., 1995, "Effect of Velocity and Temperature Distribution at the Hole Exit on Film Cooling of Turbine Blades," ASME Paper No. 95-GT-275.

Goldstein, R. J., Eckert, E. R. G., and Burggraf, F., 1974, "Effects of Hole Geometry and Density on Three-Dimensional Film Cooling," *International Journal of Heat and Mass Transfer,* Vol. 17, pp. 595–607.

Jubran, B., and Brown, A., 1985, "Film Cooling From Two Rows of Holes Inclined in the Streamwise and Spanwise Directions," ASME *Journal of Engineering for Gas Turbines and Power,* Vol. 107, pp. 84–91.

Lee, S. W., Lee, J. S., and Ro, S. T., 1994, "Experimental Study on the Flow Characteristics of Streamwise Inclined Jets in Crossflow on Flat Plate," ASME JOURNAL OF TURBOMACHINERY, Vol. 116, pp. 97–105.

Leylek, J. H., and Zerkle, R. D., 1993, "Discrete-Jet Film Cooling: A Comparison of Computational Results With Experiments," ASME JOURNAL OF TURBOMACHINERY, Vol. 116, pp. 358–368.

Makki, Z. H., and Jakubowski, G. S., 1986, "An Experimental Study of Film Cooling From Diffused Trapezoidal Shaped Holes," AIAA Paper No. 86-1326.

Pietrzyk, J. R., 1989, "Experimental Study of the Interaction of Dense Jets With a Crossflow for Gas Turbine Applications," Ph.D. Dissertation, University of Texas at Austin.

Pietrzyk, J. R., Bogard, D. G., and Crawford, M. E., 1989, "Hydrodynamic Measurements of Jets in Crossflow for Gas Turbine Film Cooling Application," ASME JOURNAL OF TURBOMACHINERY, Vol. 111, pp. 1139–145.

Schlichting, H., 1979, *Boundary Layer Theory,* McGraw-Hill, New York.

Sen, B., Schmidt, D. L., and Bogard, D. G., 1996, "Film Cooling With Compound Angle Holes: Heat Transfer," ASME JOURNAL OF TURBOMACHINERY, Vol. 118, pp. 800–806.

Subramanian, C. S., Ligrani, P. M., Green, J. G., Doner, W. D., and Kaisuwan, P., 1992, "Development and Structure of a Film-Cooling Jet in a Turbulent Boundary Layer With Heat Transfer," *Rotating Machinery Transport Phenomena, Proc. Third International Symposium on Transport Phenomena and Dynamics of Rotating Machinery (ISROMAC-3),* pp. 53–68.

Thole, K., Gritsch, M., Schulz, A., and Wittig, S., 1997, "Effect of Inlet Conditions for Jets-in-Crossflow as Applied to Film-Cooling," ASME *Journal of Fluids Engineering,* Vol. 119, pp. 533–540.

Wittig, S., Schultz, A., Gritsch, M., and Thole, K., 1996, "Transonic Film Cooling Investigations: Effects of Hole Shapes and Orientations," ASME Paper No. 96-GT-222.

Yoshida, T., and Goldstein, R. J., 1984, "On the Nature of Jets Issuing From a Row of Holes into a Low Reynolds Number Mainstream Flow," ASME *Journal of Engineering for Gas Turbines and Power,* Vol. 106, pp. 612–618.